2011 50th IEEE Conference on Decision and Control and
European Control Conference (CDC-ECC)
Orlando, FL, USA, December 12-15, 2011

A state-space view on locally-stable, globally-unstable nonlinear models driven by Gaussian burst inputs

Laurent Vanbeylen, Anne Van Mulders and Johan Schoukens

Abstract— **In this paper, the behaviour of nonlinear dynamic systems driven by stationary random excitations is studied from a model-based perspective – i.e. starting from a perfect knowledge of the system under study and its driving random input – over a finite time interval (a burst excitation is assumed). For a given discrete-time nonlinear state-space model operating in the neighbourhood of a stable equilibrium, a "blow-up" is seen as the event of escaping out of a region of attraction. Based on Laplace integration, a method is outlined to approximate a future state's probability density function (pdf) at low excitation amplitudes. Inspection of this pdf can reveal additional insights into the complex behaviour of an abstract state-space model, compared with the simulation approach. The probability of staying inside the region of attraction (viz. obtaining a bounded operation subject to an input active in a finite time interval) can be obtained by integration of this pdf. The state pdf estimation is illustrated with numerical Monte-Carlo simulation experiments.**

I. Introduction

A. Motivation of this work

Since all real-life systems are to some extent nonlinear, linear models can fail to represent their behaviour in a way satisfactory to the user. A large class of nonlinear plants can be very well approximated via the family of polynomial state-space models (with a state evolution of polynomial form in the state and input). It has good black-box approximation capabilities, and was successfully applied in practice [1]. The model can be constructed from input-output measurements of the system under study, via a least-squares data-fitting approach. The problem is that no stability guarantees are given for the resulting nonlinear state-space model; only the underlying linear dynamics are easy to analyze. It is therefore desirable to investigate (automatically) how a given state-space model behaves under a random input with predefined nature when no stability information is given. Moreover, an unstable system's state can stay within a given bounded region for very long periods of time and with a high probability (possibly not arbitrary close to one). In this paper, a method is proposed that allows one to approximate the probability distribution of a future state, given the state space equation, the initial state and the nature of the random input, consisting of a Gaussian term with known power spectrum and (if desired) a known deterministic term. Besides the randomly excited black box nonlinear model structures, possible applications include the analysis of the start-up behaviour of nonlinear oscillators, the investigation of physical (white-box) models, and controlled nonlinear plants with random noise on top of the deterministic reference signal.

This work was supported by the Fund for Scientific Research (FWO-Vlaanderen), the Flemish Government (Methusalem Grant METH-1) and the Belgian Program on Inter-university Poles of Attraction initiated by the Belgian State, Prime Minister's Office, Science Policy programming (IAP VI/4 - Dysco).

All authors are with the Department ELEC, Vrije Universiteit Brussel, Pleinlaan 2, B-1050 Brussel, Belgium. Email: Laurent.Vanbeylen@vub.ac.be

B. Example of locally stable, globally unstable dynamics

The time interval over which a bounded response is observed for unstable systems depends both on the system itself and on the stochastic input's properties [2]. Nonlinear models' responses (starting from rest) can, e.g., be bounded (this behaviour can appear "stable") for long periods of time at low input amplitudes (variance for stochastic inputs), and at high amplitudes only remain bounded for short periods of time, revealing the true unstable nature of the system. For the amplitude levels in between, there can be a transition, with a decrease of the typical time over which the response remains bounded as function of the input variance. This kind of effect can be expected with state space systems with a state transition function of the form $f(x,u) = Ax + Bu + o(x) + o(u)$ (where u is the input and x is the state) with eigenvalues of the A matrix lying in the open unit disk, i.e., nonlinear systems having asymptotically stable underlying linear dynamics. If both the input and the state vector are small, the $o()$-term vanishes; as a result, the origin is a locally stable equilibrium of the unforced system (autonomous, $u = 0$). The autonomous system's response is a given deterministic state trajectory. In this sense, a nonzero random input causes state fluctuations. Inside a so-called Region Of Attraction (ROA) around the equilibrium point, the state is attracted towards the equilibrium in the unforced (i.e. zero input) situation. Outside, the nonlinear terms can become very active and cause the state to be repelled away from the origin.

C. Towards a concrete problem setting

In this context, the practical goal is to quantify the "risk" for the state to leave a certain domain $\mathcal{D}$ in a given period of time, say, of τ samples, for a specified random excitation. In this work, we restrict ourselves to the case of a known model equation, initial state and colored Gaussian input with known power spectrum. To achieve this goal, we propose in this chapter to calculate the probability density function (pdf) of the state at time τ. If the pdf is integrated over a domain $\mathcal{D}$ chosen as the ROA [3], [4], the probability is obtained for the state to be asymptotically attracted to the equilibrium after a burst of τ noise samples (followed by a zero input).

This will be called bounded operation over a time interval of length τ (to be defined in the sequel). The reader may comment that the state pdf at time τ can also be estimated from Monte-Carlo simulations of the system. One advantage of the method to be presented, is that it obtains a much better accuracy in low pdf regions, where a Monte-Carlo simulation hardly ever turns up. A second advantage is that the results for a range of standard deviations can be obtained, at almost no additional computational cost.

D. Related literature on stability and randomly excited systems

Several theoretical notions have been introduced to describe the stability of a model with external input, such as input-output stability [5] and input-to-state stability (ISS; see [6], [7]). The stability proofs for nonlinear systems are usually established on a case-by-case basis (mostly via a Lyapunov function). These concepts can guarantee bounds on the state's magnitude, consisting of a term coming from the bounded input (which has to be piecewise continuous in the continuous-time setting) and a term vanishing over time depending on the initial state. Due to its unboundedness, a random input with an infinite (amplitude) support does not fit into the classical ISS framework (the state upper bound in ISS degenerates to infinity); ISS has also a stochastic counterpart in continuous-time, requiring Itô stochastic calculus, in which the state upper bound holds with probability arbitrary close to one (stability in probability, [8]). However, as the other notions of stability, this concept remains theoretical and is hard to apply.

To our best knowledge, the most closely related work in the literature is the monograph by [9], giving a quite theoretical and mathematically deep treatment of the problem of continuous-time dynamical systems subject to random perturbations (requiring advanced functional calculus), and introducing interesting notions as escape probability, mean exit time and most probable exit path. Besides, the optimal path concept is studied for systems driven by Gaussian noise in [10], focusing on the prehistory rather than the future.

In this contribution, the model is discrete in time, the input fluctuations on top of the deterministic input are assumed to be colored and Gaussian. We focus on the calculation of the pdf of $x(\tau)$, without needing to simulate the model's response extensively and explicitly. Doing so, it can e.g. be seen which regions of the state space are very unlikely to be visited on the time scale τ. Since instability is inherently a transient phenomenon, and initially the state can stay inside a ROA for long periods of time, it is therefore interesting to consider the state's distribution after a finite time in the future. Moreover, due to the instability, the state response to a stationary input (without deterministic term) is not stationary. In the locally stable situation, up to the initial transient and before the leaving the ROA, it just appears as a stationary random sequence.

E. Main contributions and organization

The main contributions of this paper are the following:

- (theoretical) calculation of a future state's pdf as a multivariate integral involving Dirac delta distributions;
- reformulation of the dominant contributions to the integral as a constrained optimization problem, providing an interpretation of its solution;
- evaluation via a variant of the Laplace Integration Method;
- verification of the theoretical results by means of a Monte-Carlo simulation example.

This paper is organized as follows. In Section II, the assumptions are formalized. In Section III, the state's pdf approximation is presented. Finally, Section IV shows the results of Monte-Carlo simulations illustrating the method.

II. Assumptions

Assumption 1: (the class of discrete-time state-space models considered)

In the state evolution equation

$$x(t+1) = f(x(t), u(t)) \tag{1}$$

with $x(t) \in \mathbb{R}^n$ ($n \in \mathbb{N}_0$ is called the model order), $u(t) \in \mathbb{R}$, the function $f(\bullet, \bullet)$ is a known continuously differentiable function w.r.t. both arguments.

Assumption 2: (initial state)

The initial state $x(0)$ is known.

To allow for an interpretation as a probability of unbounded operation, a ROA is assumed to exist and to be compact. Therefore, it is also assumed that the origin is an asymptotically stable and isolated equilibrium point of (1) for $u(t) = 0$.

Note that the procedure also applies for non-state-affine and non-input-affine state equations.

Assumption 3: (stochastic framework)

The input $u(t)$ consists of the superposition

$$u(t) = u_0(t) + n_u(t) \tag{2}$$

of a known deterministic term $u_0(t)$ (defined on the time interval $t \in [0, \tau - 1]$) and a zero-mean, stationary, colored Gaussian noise term $n_u(t)$ with known power spectrum $S_{uu}(\omega)$, and with ω the (normalized, discrete-time) angular frequency. Translated into the frequency domain, this means that the kth frequency component (normalized Discrete Fourier Transform $\frac{F_\tau}{\sqrt{\tau}}$, as defined below, and denoted DFT for short) of $u(t)$, U_k, is circular complex normally distributed [11]

$$U_k \sim N_C(U_{0,k}, \sigma_k^2) \tag{3}$$

with $U_{0,k}$ the DFT of $u_0(t)$, $\sigma_k^2 = S_{uu}(\omega_k) > 0$ the (total complex) variance, and ω_k the angular frequency at frequency line k.

Throughout, the (total) time domain variance will be denoted as σ_U^2.

Please notice that, by this assumption, the input signal is automatically real (and hence never infinite) with probability one on $t \in [0, \tau - 1]$. As a second remark, it can be said that a zero input power spectrum is not allowed, since

it can create problems further on when it appears in the denominator.

A. Consequence: bounded operation over a time interval of length τ

Assuming (i) that the ROA of the origin exists in the unforced situation, viz.

$$\text{ROA} = \left\{ x(0) \in \mathbb{R}^n \mid \lim_{t\to\infty} x(t) = 0 \text{ with } x(t+1) = f(x(t),0) \right\}$$

and (ii) that the input is a burst of length τ, viz. $u(t) = 0,\ t > \tau$, the probability to obtain a state finally converging towards the (isolated) asymptotic equilibrium point at the origin under all above-mentioned assumptions equals the state's pdf at time τ integrated over the ROA:

$$\int_{\text{ROA}} p_{x(\tau)}(x)dx \tag{4}$$

Note that the state may escape the ROA during the first $\tau - 1$ samples, as long as it comes down into it before the time interval has come to an end. In the unforced situation, initial states not contained into the ROA can – besides drift away to infinity – also be attracted to other equilibria (fixed points), limit cycles, periodic solutions or chaotic "strange" attractors. If all these phenomena are considered as undesired behaviour, the probability for undesired behaviour is the complement of the above-defined probability (4).

III. Estimation of the state's probability distribution

This section contains the core material of this contribution, which is the estimation of the state's probability distribution at time instant $\tau \in \mathbb{N}_0$ under the above assumptions. The probability density function (pdf) $p_{x(\tau)}(x(\tau))$ of the state $x(\tau)$ can be calculated as the integrated form of a higher-dimensional joint pdf based on all states and inputs:

$$p_{x(\tau)}(x(\tau)) = \int_{-\infty}^{+\infty} p_{\mathbf{x},x(\tau),\mathbf{u}}(\mathbf{x}, x(\tau), \mathbf{u}) d\mathbf{x} d\mathbf{u} \tag{5}$$

with $\mathbf{x}^T = \begin{bmatrix} x(1)^T & \dots & x(\tau-1)^T \end{bmatrix} \in \mathbb{R}^{(\tau-1)n}$ and $\mathbf{u}^T = \begin{bmatrix} u(0) & \dots & u(\tau-1) \end{bmatrix} \in \mathbb{R}^{\tau}$ the intermediate states and inputs respectively. The integrand can be rewritten as

$$p_{\mathbf{x},x(\tau),\mathbf{u}}(\mathbf{x}, x(\tau), \mathbf{u}) = p_{\mathbf{u}}(\mathbf{u})\, p_{\mathbf{x},x(\tau)|\mathbf{u}}(\mathbf{x}, x(\tau), \mathbf{u}) \tag{6}$$

with $p_{\mathbf{u}}(\mathbf{u})$ a known Gaussian pdf based on Assumption 3, and $p_{\mathbf{x},x(\tau)|\mathbf{u}}$ the conditional distribution of the states given the input sequence. Since in any case, the initial state is always known, the states are deterministic in $p_{\mathbf{x},x(\tau)|\mathbf{u}}$, which becomes a multivariate Dirac delta distribution imposing each state evolution equation (1) at $t = 0 \dots \tau - 1$.

A. Detailed specification of the integrand: both factors in (6)

The first factor is given by

$$p_{\mathbf{u}}(\mathbf{u}) = (\det 2\pi\Sigma_{\mathbf{u}})^{-1/2} \exp\left(-\frac{1}{2} (\mathbf{u} - \mathbf{u}_0)^T \Sigma_{\mathbf{u}}^{-1} (\mathbf{u} - \mathbf{u}_0) \right) \tag{7}$$

with deterministic part $\mathbf{u}_0^T = \begin{bmatrix} u_0(0) & \dots & u_0(\tau-1) \end{bmatrix}$.

Using the Whittle approximation (combination of Toeplitz-circulant properties and the Wiener-Khinchin theorem), it can be shown that

$$(\mathbf{u} - \mathbf{u}_0)^T \Sigma_{\mathbf{u}}^{-1} (\mathbf{u} - \mathbf{u}_0) \approx \varepsilon^H \varepsilon \tag{8}$$

with

$$\varepsilon = \text{diag}\left(\mathbf{S}_{uu}^{-1/2} \right) \frac{F_\tau}{\sqrt{\tau}} (\mathbf{u} - \mathbf{u}_0) \tag{9}$$

and $F_\tau = \left[\exp\left(-j\frac{2\pi}{\tau} kl \right) \right]_{k,l=0\dots\tau-1} \in \mathbb{C}^{\tau\times\tau}$, $\mathbf{S}_{uu} = \left[S_{uu}(\omega_k) \right]_{k=0\dots\tau-1} = \left[\sigma_k^2 \right]_{k=0\dots\tau-1}$. This means that the signal $\mathbf{u} - \mathbf{u}_0$ has simply to be Discrete Fourier Transformed and scaled frequency by frequency to obtain ε, which can be interpreted as "driving" white noise.

The second factor is given by

$$p_{\mathbf{x},x(\tau)|\mathbf{u}} = \prod_{t=0}^{\tau-1} \delta\left(f(x(t), u(t)) - x(t+1) \right) \tag{10}$$

with $\delta(x)$ the multivariate Dirac delta distribution. Since a Dirac delta distribution only has nonzero contributions at the places where its argument is nonzero, one observes that this second factor introduces a constraint on the integration variables (states and inputs).

B. Performing the integration

The careful reader could wonder how the high-dimensional integration containing Dirac distributions in (5) can be performed. Let us first observe that (5) only has contributions at the places where the argument of each Dirac delta is zero, and consists of at least as many integration variables ($(\tau-1)n + \tau$) as constraints implied by these Dirac delta's ($n\tau$) if $\tau \geq n$, which is the nontrivial case – otherwise the integral would be zero. If the constraints are nowhere satisfied (this situation corresponds to a non-controllability of the model), then the integral vanishes too.

Now we briefly (due to space limitations we cannot go into full detail here) explain how one can proceed with the (approximate) integration of the integrand with a Dirac delta distribution of the form

$$I = \int_{-\infty}^{+\infty} e^{-\gamma V(\eta)} \delta(\Psi(\eta))\, d\eta \tag{11}$$

First, local linear and quadratic Taylor approximants are formed to Dirac's operand $\Psi(\eta)$ (corresponding to $f(x(t), u(t)) - x(t+1)$ in vector form) and the exponent $V(\eta)$ (corresponding to the quadratic form (8), up to a scalar factor denoted γ) respectively. Then the integral is approximated by using the approximants instead of the functions themselves. Then, the Delta distribution can be

eliminated, and, due to the quadratic form in the exponent, the resulting integral can be viewed as the normalization constant of a multivariate Gaussian pdf, which is analytically known (the obtention of the quadratic form combined with the Gaussian pdf idea is known as Laplace's integration method [12]). Notice that the scaling of γ and $V(\eta)$ in the left hand side of $\gamma V(\eta) = (\mathbf{u}-\mathbf{u}_0)^T \Sigma_{\mathbf{u}}^{-1} (\mathbf{u}-\mathbf{u}_0)$ is fixed by viewing γ as the inverse of the input variance σ_U^2

$$\gamma = \sigma_U^{-2} \tag{12}$$

The local expansions can be motivated as follows. The integrand is, in the subspace satisfying Dirac's constraint, dominant at the minimizer of $V(\eta)$, denoted η^*. A decrease to zero of the input variance, corresponding to an increase to infinity of the parameter γ in (11), tends to reduce the region of "activity" of the integrand to a small neighbourhood (on the constraint subspace) of the constrained minimizer of $V(\eta)$. As a consequence, the integral approximation error tends to zero as the input variance tends to zero. Moreover, in this specific situation (integral (5)), due to the quadratic property of $V(\eta)$, this error only comes from the local linearization of the nonlinear function in $\Psi(\eta)$.

C. Interpretation

Interesting to report is the interpretation of the constrained minimizer η^*

$$\eta^* = \underset{\substack{\eta \\ \text{s.t. } \Psi(\eta)=0}}{\operatorname{argmin}} V(\eta) \tag{13}$$

the neighbourhood of which is contributing the most to the integral representing $x(\tau)$'s pdf. The variable η corresponds to the integration variables, which are the concatenation of the states $\mathbf{x}$ and inputs $\mathbf{u}$. The constrained optimization problem, translated in these terms, reads

$$\underset{\substack{\mathbf{x},\mathbf{u} \\ \text{s.t. } x(t+1)=f(x(t),u(t))}}{\operatorname{argmin}} (\mathbf{u}-\mathbf{u}_0)^T \Sigma_{\mathbf{u}}^{-1} (\mathbf{u}-\mathbf{u}_0) \tag{14}$$

Due to the fulfillment of the constraints, η^* coincides with a state-input combination that satisfies the state equation at each time instant, and the state trajectory obtained starts at the initial state $x(0)$ and it ends at the argument $x(\tau)$ of the pdf $p_{x(\tau)}(x(\tau))$. Due to the minimization of the quadratic form, we conclude, in the Gaussian case, that the normalized input energy (normalized with the specified input power spectrum) of η^* has to be minimal. In general, even if the pdf is not Gaussian, the input signal of η^* can be interpreted as the most likely one (maximization of $p_{\mathbf{u}}(\mathbf{u})$) that drives the state of η^* on a trajectory from $x(0)$ to the point of evaluation of $p_{x(\tau)}$.

D. Putting theory into practice

Applying the theoretical results (not presented here) to the estimation of (5) involves $n_\eta = (\tau-1)n+\tau$ integration dimensions (related to the concatenation of $\mathbf{x}$ and $\mathbf{u}$), and $n_\Psi = n\tau$ constraint dimensions (related to the state evolution at each time instant). Then the integration variables are to be split up in two parts, η_1 and η_2, the first of which is of dimension n_Ψ. The choice is made to let η_1 correspond to $x(1),\ldots,x(\tau-1),u(0),\ldots,u(n-1)$ and η_2 to $u(n),\ldots,u(\tau-1)$. The respective columns of Ψ's Jacobian, evaluated at η^*, are then used to define the sparse matrices J_1^* and J_2^* ($\frac{\partial \Psi}{\partial \eta}|_{\eta^*} = \begin{bmatrix} J_1^* & J_2^* \end{bmatrix}$). The constrained minimization (14) can be achieved via, e.g., Lagrange-Newton algorithms, and involves a Fast-Fourier-Transform-based implementation combined with sparse matrices. Not forgetting the first factor of (7), the approximation of the pdf's logarithm (obtained via Laplace integration) becomes,

$$\log I \approx -\log|\det J_1^*| - \gamma V(\eta^*) + \frac{\Delta n}{2}\log 2\pi - \frac{1}{2}\log|\det \gamma H_W| \tag{15}$$

in which $\Delta n = n_\eta - n_\Psi$, and

$$H_W = \begin{bmatrix} -J_1^{*-1}J_2^* \\ I^{\Delta n \times \Delta n} \end{bmatrix}^T \frac{\partial^2 V}{\partial \eta^2} \begin{bmatrix} -J_1^{*-1}J_2^* \\ I^{\Delta n \times \Delta n} \end{bmatrix} \tag{16}$$

(with identity matrices $I^{\Delta n \times \Delta n}$) can be rewritten as:

$$\begin{array}{c} \log p_{x(\tau)}(x(\tau)) \approx -\frac{n}{2}\log 2\pi - \frac{1}{2}\log|\det \Sigma_{\mathbf{u}}| - \log|\det J_1^*| \\ -\frac{1}{2}(\mathbf{u}-\mathbf{u}_0)^T \Sigma_{\mathbf{u}}^{-1}(\mathbf{u}-\mathbf{u}_0) - \frac{1}{2}\log|\det \gamma H_W| \end{array} \tag{17}$$

Remark. The pdf at another input variance can be obtained with almost no additional computational effort (the optimization problem, and so its solution, remain the same, just a slight modification of the constants in the pdf's expression is needed at the places where a γ or covariance matrix is present).

IV. Simulation results

The present implementation is based on the Matlab's nonlinear constrained optimization routine `fmincon`, and uses an interior point algorithm (iteration step computed via conjugated gradients, Hessian calculated via finite differences, analytically calculated gradients of cost and constraint functions, and a constraint tolerance of 10^{-13}). The method is illustrated by means of 2-dimensional examples, since this allows graphical representations of the pdf.

The following continuous-time state equation, formulated in polar coordinates (ρ,ϕ), is considered:

$$\dot{\rho} = -\rho(1-\rho^2) \tag{18}$$

$$\dot{\phi} = 1 \tag{19}$$

It has as ROA the region $\rho < 1$ located inside the unit circle (all initial states inside get attracted to the origin, while those starting outside get repelled, towards infinity). This is easily seen from the sign of the function $-\rho(1-\rho^2)$ changing at $\rho = 1$, and the decoupling of both coordinates. Writing in Cartesian coordinates and adding a linear input-term, one obtains

$$\dot{x} = -x(1-x^Tx) + \begin{bmatrix} 0 & -1 \\ 1 & 0 \end{bmatrix} x + Bu$$

Inspired by this continuous-time system, the discrete-time system given by Euler discretization of the former is introduced:

$$f(x,u) = x + T_s\left(-x(1-x^Tx) + \begin{bmatrix} 0 & -1 \\ 1 & 0 \end{bmatrix} x + Bu\right)$$

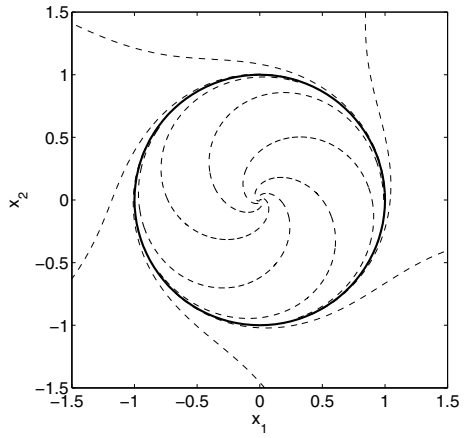

Fig. 1. Phase portrait of the autonomous system under consideration (dashed lines). The states rotate counterclockwise. The ROA is the region located inside the unit circle (bold curve). Initial states inside the unit disk get attracted towards the origin, while initial states starting outside tend towards infinity.

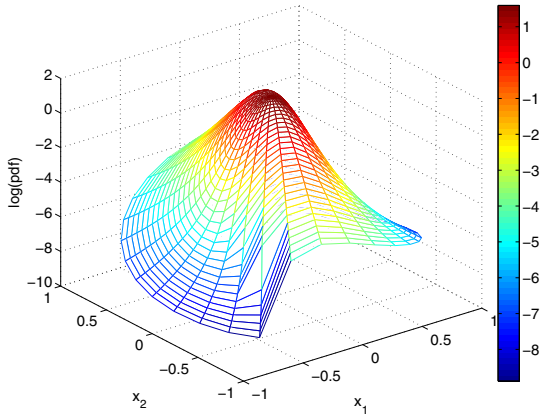

Fig. 2. (Naperian) logarithm of the estimated pdf $p_{x(\tau)}$.

with $T_s = 0.01$. We let the method estimate the pdf for $\tau = 300$, a Gaussian input with time-domain standard deviation $\sigma_U = 3$ (white power spectrum), $x(0) = \begin{bmatrix} 0 & 0 \end{bmatrix}^T$, $u_0(t) = 0$ ($\forall t = 0 \ldots \tau - 1$), $B = \begin{bmatrix} 1 & 1 \end{bmatrix}^T$. A grid over the ROA (which is here the unit disk), parameterized in polar coordinates, was chosen with 30 linearly spaced ρ-values and 30 linearly spaced ϕ-values. Each grid point requires a constrained optimization.

A. Nonlinear model equations

Figures 2 and 3 show respectively the pdf's (naperian) logarithm, and the location of the state $x(\tau)$ for 1500 Monte-Carlo runs (using a Gaussian input satisfying the assumptions) shown on top of the pdf logarithm's contour plot. The pdf shows how the states $x(\tau)$ are distributed at time τ. The distribution of the random Monte-Carlo realizations of the states is in good agreement with the estimated pdf. It is seen that the pdf deviates from a Gaussian distribution and the contour lines are not elliptical (the pdf's logarithm clearly deviates from a paraboloid). This indicates that, although a linearization took place in the method, the method still

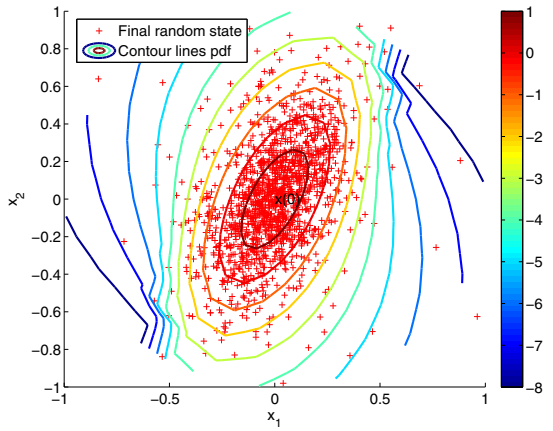

Fig. 3. Contour lines of the logarithm of $p_{x(\tau)}$, with a scatter plot of random Monte-Carlo values of the state $x(\tau)$ indicated with crosses. Notice the excellent agreement between both. The major axis of the approximately elliptical contour lines around the origin is slightly rotated compared with the diagonal axis along which the input enters into the state ($B = \begin{bmatrix} 1 & 1 \end{bmatrix}^T$); this is due to the natural rotation in the phase plane induced by $\dot{\phi} = 1$.

grasps some nonlinear behaviour. The method allows one to predict which regions are less likely locations of the state $x(\tau)$, without requiring extensive simulation efforts as would be the case with a purely Monte-Carlo approach. Based on this mesh, a 2-dimensional Simpson integration of the pdf over the ROA returns as probability of bounded operation over a time interval of length τ ($\mathbb{P}(x(\tau) \in \text{ROA})$) the value 98.53% (the integration error is approximately 0.1%). This can be compared with the value 97.27% (with estimated standard deviation of 0.42%) obtained from the fraction of Monte-Carlo simulations resulting in a state $x(\tau)$ in the ROA. The 95% confidence-interval does not contain the estimated value, indicating a small mismatch between both values. This has probably to do with the violation of the assumption that the input should have a small standard deviation. Anyway, the method clearly succeeds in providing an order of magnitude of the risk of leaving the ROA, which is the complement of the above-mentioned probability values: 1.47%±0.1% against 2.73%±0.84% (2σ-confidence). Performing a linear analysis with the underlying linear system, would result in a severe underestimation of the risk $\mathbb{P}(x(\tau) \notin \text{ROA}) = 0.03\%$. In addition, it can be mentioned that the whole procedure on this mesh (run on a PC with a 2.0 GHz Intel Xeon with 4.0 GB RAM), takes less than 8 minutes of computation time.

B. Gathering information at other input standard deviation values

Another advantage of the method is that it allows one to estimate the probability of stable operation also at other input standard deviation values at once, without needing to solve additional constrained optimization problems (just the constants in the pdf expressions are changing). Figure 4 shows the estimated probabilities of stable operation, both in the nonlinear case and in the linear case, and compared with

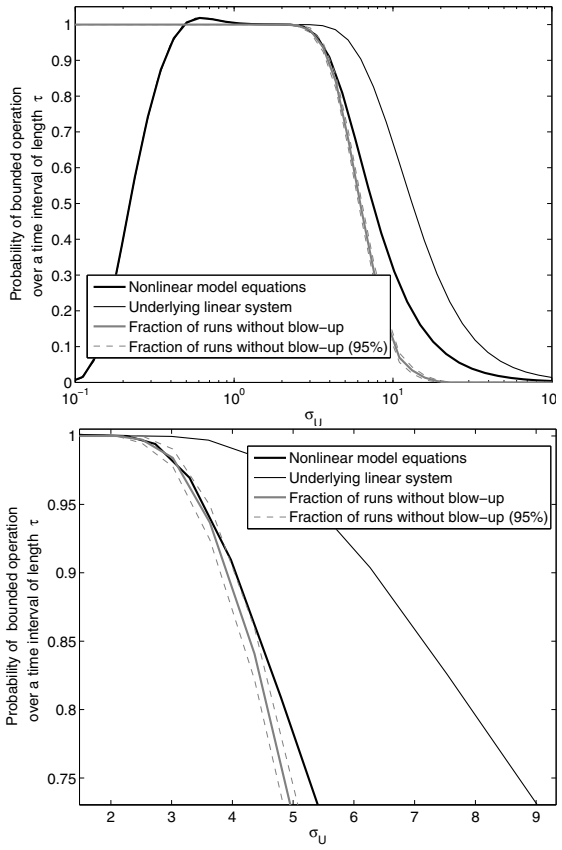

Fig. 4. Top figure: Estimated probabilities of stable operation over a time interval of length τ, both in the nonlinear case and in the linear case. Notice that the part of the graph below $\sigma_U = 2$ is not reliable, since the integration grid has not been modified, while the pdf concentrates more around the origin (serious integration errors are taking place). Notice the underestimation of the risk of leaving the ROA when the underlying linear model is used. The results are compared with the fraction of 1500 Monte-Carlo runs of length τ resulting in a bounded behaviour (grey line; the 95% confidence interval is shown with a dashed grey line). Bottom figure: detail.

the results of 1500 Monte-Carlo simulations of length τ. The limitation of this method is as follows: at small σ_U-values a discrepancy occurs between the true probabilities (very close to 1) and the estimated one (cf. the part of the figure corresponding to $\sigma_U < 2$). This is due to the integration grid, which is not well matched to the fast variations of the pdf around the origin at low σ_U-values. In the region $2 < \sigma_U < 4.5$, a reasonable approximation is obtained.

V. Conclusions

In this paper, given the input's deterministic part, the power spectrum of the Gaussian part, the analytic form of the state evolution equation, and the initial state, the pdf of a future state was calculated as an integral and using Bayes' rule. If the input variance is small, the (very high dimensional) integral can be well approximated at any point of the state space via the Laplace integration method. This, in turn, requires the solution of a constrained optimization problem, which can be interpreted as the most likely scenario (trajectory) driving the state from its initial position to the pdf's argument. The constrained optimization involves sparse matrices. A few options for the generation of initial estimates to the nonlinearly constrained optimization problem have been presented. The problem setting (model equation, input noise and initial state) can be extended and generalized in different ways. A theoretical analysis of the integration error shows that it essentially depends on the magnitude of second derivatives of the state equation. If the input is a finite-time burst, one obtains the probability of getting asymptotically attracted towards the origin via the integral of the pdf over the region of attraction of the unforced system. The proposed method provides more insight and is more efficient to estimate the pdf than a brute-force simulation approach, especially in the regions where the pdf is very low, since this could require a huge number of simulations to get an accurate result. Another advantage compared with the Monte-Carlo approach, is that the pdf computations at other input standard deviations can be performed at once, without needing to solve additional constrained optimization problems. Simulation results are shown to illustrate and support the theory. Although the estimated probability of bounded operation is not always perfectly correct, due to the fact that the input standard deviation is not (very) small as assumed in the theory, a correct order of magnitude is obtained, outperforming a classical analysis of the underlying linear dynamics, which would result in a severe underestimation of the risk. The optimization of the choice of the integration method and of the density of the integration grid, is left for future research.

References

[1] J. Paduart, L. Lauwers, J. Swevers, K. Smolders, J. Schoukens, and R. Pintelon, "Identification of nonlinear systems using polynomial nonlinear state space models," *Automatica*, vol. 46, no. 4, pp. 647–656, 2010.

[2] L. Vanbeylen, J. Schoukens, and K. Barbé, "Measuring the stability of nonlinear feedback systems," in *2008 IEEE Instrumentation & Measurement Technology Conference Proceedings*, Victoria, Canada, May 2008, pp. 922–927.

[3] S. Balint, E. Kaslik, A. Balint, and A. Grigis, "Methods for determination and approximation of the domain of attraction in the case of autonomous discrete dynamical systems," *Advances in Difference Equations*, vol. 2006, no. ID23939, pp. 1–15, 2006.

[4] A. Zečević and D. Šiljak, "Regions of Attraction," *Control of Complex Systems*, pp. 111–141, 2010.

[5] H. Khalil, *Nonlinear systems*. Upper Saddle River (NJ), USA: Prentice Hall, 2002.

[6] E. Sontag, "Input to state stability: Basic concepts and results," *Nonlinear and Optimal Control Theory*, vol. 1932/2008, pp. 163–220, 2008.

[7] Z. Jiang and Y. Wang, "Input-to-state stability for discrete-time nonlinear systems," *Automatica*, vol. 37, no. 6, pp. 857–869, 2001.

[8] S. Liu, J. Zhang, and Z. Jiang, "A notion of stochastic input-to-state stability and its application to stability of cascaded stochastic nonlinear systems," *Acta Mathematicae Applicatae Sinica (English Series)*, vol. 24, no. 1, pp. 141–156, 2008.

[9] M. Freidlin and A. Wentzell, *Random perturbations of dynamical systems*. New York (NY), USA: Springer, 1998.

[10] M. Dykman and V. Smelyanskiy, "Distribution of fluctuational paths in noise-driven systems," *Superlattices and Microstructures*, vol. 23, pp. 495–504, 1998.

[11] B. Picinbono, *Random signals and systems*. Prentice Hall, 1993.

[12] N. de Bruijn, *Asymptotic methods in analysis*, 3rd ed. Amsterdam, The Netherlands: North Holland, 1970.